Polymer Chemistry

www.rsc.org/polymers

Volume 4 | Number 3 | 7 February 2013 | Pages 417–852

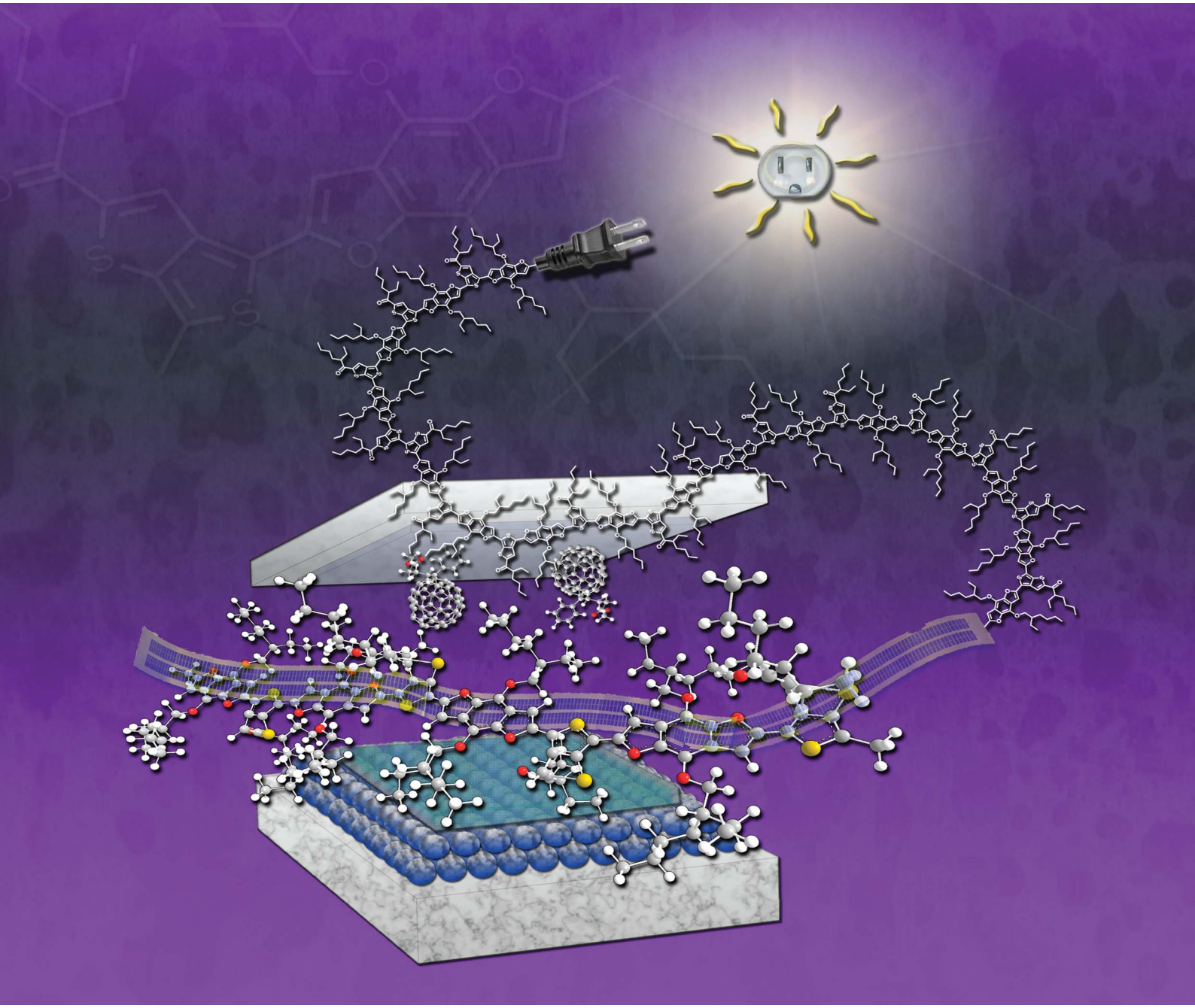

ISSN 1759-9954

RSC Publishing

PAPER

Yingping Zou, Yongfang Li *et al.*

A benzo[1,2-*b*:4,5-*b*′]difuran- and thieno-[3,4-*b*]thiophene-based low bandgap copolymer for photovoltaic applications

1759-9954(2013)4:3;1-K

Polymer Chemistry

RSC Publishing

PAPER

View Article Online
View Journal | View Issue

Cite this: *Polym. Chem.*, 2013, **4**, 470

A benzo[1,2-*b*:4,5-*b*′]difuran- and thieno-[3,4-*b*]thiophene-based low bandgap copolymer for photovoltaic applications†

Bo Liu,[ab] Xuewen Chen,[b] Yingping Zou,*[abc] Yuehui He,[a] Lu Xiao,[b] Xinjun Xu,[d] Lidong Li[d] and Yongfang Li*[e]

Received 30th July 2012
Accepted 10th September 2012

DOI: 10.1039/c2py20580g

www.rsc.org/polymers

A new low bandgap conjugated polymer—PBDFTT-C was synthesized from thieno-[3,4-*b*]thiophene and benzo[1,2-*b*:4,5-*b*′]difuran units by Stille coupling reactions. The structure was verified by ^{1}H NMR and elemental analysis, the molecular weight was determined by gel permeation chromatography (GPC) and the thermal properties were investigated by thermogravimetric analysis (TGA). PBDFTT-C showed a low HOMO energy level of −5.27 eV. The polymer film displayed broad absorption in the wavelength region from 300 nm to 840 nm with a low bandgap of 1.48 eV. The field effect hole mobility of PBDFTT-C reached 5.4 × 10^{-3} cm^2 V^{-1} s^{-1}. By using 1,8-diiodooctane (DIO) as the solvent additive, photovoltaic cells with the structure of ITO/PEDOT:PSS/PBDFTT-C:$PC_{71}BM$ (1 : 1.5, w/w)/Ca/Al demonstrated a power conversion efficiency of 4.4% with a short circuit current of 10.45 mA cm^{-2}, open circuit voltage of 0.66 V and a fill factor of 0.64, under the illumination of AM 1.5G, 100 mW cm^{-2}.

Introduction

Polymer solar cells (PSCs) based on solution-processable conjugated polymer donors and fullerene derivative acceptor materials have attracted much attention in both academia and industry in recent years, with their performances increasing significantly.[1–3] The power conversion efficiency (PCE) of bulk heterojunction (BHJ) PSCs has reached up to 8% from *ca.* 1% in 2000.[4] The improved performance benefited from the optimized device fabrication conditions and the development of new semiconducting polymer donor and fullerene derivative acceptor photovoltaic materials.[5–8]

In recent years, alternating copolymerization has been broadly used to synthesize promising polymer donors because of its fine tuning of the bandgap, absorption spectra and energy levels.[9–13] The thieno-[3,4-*b*]thiophene (TT) unit with a strong electron-withdrawing substituent is a typical building block used in low bandgap conjugated polymers for high efficiency PSCs, and many TT based conjugated polymers with different electron donor units, such as benzo[1,2-*b*:4,5-*b*′]dithiophene (BDT), exhibited excellent photovoltaic properties.[14]

Very recently, benzo[1,2-*b*:4,5-*b*′]difuran (BDF) based polymers as electron donors were used in PSCs and demonstrated promising photovoltaic properties. For example, Huo *et al.* reported a copolymer (PBDFDTBT) with a high PCE up to 5% after thermal annealing, this was the first publication about a BDF based polymer for photovoltaic applications.[15] Moreover, we also synthesized a new BDF-based polymer (PBDFNTDO) and PSC devices based on PBDFNTDO as the donor and $PC_{71}BM$ as the acceptor showed a high PCE of 4.71% without any post-treatment.[16]

Based on the above considerations, the development of new low bandgap BDF based copolymers with TT as the copolymerizing unit should therefore lead to some interesting features for photovoltaic applications. Herein, a new copolymer, poly{4,8-bis(2-ethylhexyloxy)benzo[1,2-*b*;3,4-*b*′]difuran-*alt*-thieno-[3,4-*b*]thiophen-2-yl)-2-ethylhexan-1-one} (PBDFTT-C), was synthesized by Stille coupling reactions. The polymer was soluble in common organic solvents. The polymer film exhibited broad absorption in the wavelength region from 300 nm to 840 nm. Polymer solar cells with the configuration of ITO/PEDOT:PSS/PBDFTT-C:$PC_{71}BM$ (1 : 1.5, w/w)/Ca/Al and 1,8-diiodooctane (DIO, 3 vol%) as an additive demonstrated a promising power conversion efficiency of 4.4% under the

[a]*State Key Laboratory for Powder Metallurgy, Central South University, Changsha 410083, China. E-mail: yingpingzou@csu.edu.cn*

[b]*College of Chemistry and Chemical Engineering, Central South University, Changsha 410083, China*

[c]*Institute of Super Microstructure and Ultrafast Process, Central South University, Changsha 410083, China*

[d]*School of Materials Science and Engineering, University of Science and Technology Beijing, Beijing 100083, China*

[e]*Beijing National Laboratory for Molecular Sciences, Institute of Chemistry, Chinese Academy of Sciences, Beijing 100190, China. E-mail: liyf@iccas.ac.cn*

† Electronic supplementary information (ESI) available: Fig. S1 gives the GPC spectrum of the PBDFTT-C, Fig. S2 gives the output and transfer characteristics of the PBDFTT-C thin films, Table S1 gives the FET data of PBDFTT-C. Fig. S3 and S4 give the *J–V* curves from the devices with some modifications and EQE curves. Table S2 gives the corresponding photovoltaic data. See DOI: 10.1039/c2py20580g

illumination of AM 1.5G, 100 mW cm^{-2}. A hole mobility of 5.4 $\times 10^{-3}$ cm^2 V^{-1} s^{-1} for PBDFTT-C was obtained in organic field effect transistors (OFETs).

Experimental section

Materials

Furan-3-carboxylic acid, *n*-butyllithium (*n*-BuLi), tetrakis-(triphenylphosphine)palladium ($Pd(PPh_3)_4$) and trimethyltin chloride ($Sn(CH_3)_3Cl$) were obtained from Acros Organics, and they were used as received. Toluene was dried over P_2O_5 and freshly distilled prior to use. Other reagents and solvents were purchased commercially as ACS-grade quality and used without further purification. 1-(4,6-Dibromothieno[3,4-*b*]thiophen-2-yl)-2-ethylhexan-1-one (M1)[17] was prepared according to the reported procedure. 2,6-Bis(trimethyltin)-4,8-bis(2-ethylhexyloxy)benzo[1,2-*b*;3,4-*b*′]difuran (M2) was synthesized as we described before.[16]

Characterization

^{1}H NMR spectra were recorded using a Bruker DMX-400 spectrometer, chemical shifts were reported as δ values (ppm) relative to an internal tetramethylsilane (TMS) standard. Number-average (M_n) and weight-average (M_w) molecular weights were measured by the gel permeation chromatography (GPC) method, using polystyrene as a standard. TGA was performed on a PE TGA-7 at a heating rate of 20 K min^{-1} under a nitrogen atmosphere. UV-vis absorption spectra were taken using a Hitachi U-3010 UV-vis spectrophotometer. For solid state measurements, polymer solution in chloroform was cast on quartz plates. Cyclic voltammograms (CV) were recorded on a CHI 660C (China) Electrochemical Workstation using a platinum disk coated with the polymer film, Pt wire and a Ag/AgCl electrode in an anhydrous and argon-saturated solution as the working electrode, counter electrode and reference electrode respectively in a 0.1 mol L^{-1} tetrabutylammonium hexafluorophosphate (Bu_4NPF_6) acetonitrile solution at a scan rate of 50 mV s^{-1}. AFM images were obtained using a Veeco's Dimension V atomic force microscope (AFM) in the tapping mode.

Fabrication of organic field-effect transistors

Organic field-effect transistors (OFETs) were fabricated with a bottom-gate top-contact configuration. Thermally oxidized (100) silicon wafers (n^{++} doped) with a SiO_2 thickness of 300 nm were sequentially cleaned with detergent, deionized water, acetone and ethanol in an ultrasonic bath. Then hydrophilic treatment of these silicon wafers was performed by soaking the substrates in a mixture of deionized water, 25% ammonium hydroxide and 30% H_2O_2 (5 : 1 : 1 by volumetric ratio) for 20 min at 80 °C followed by rinsing with deionized water and dried with nitrogen flow. A octadecyltrimethoxysilane self-assembled monolayer modified organic film was selected as a dielectric modification layer in the OFETs according to the reported method.[18] The conjugated polymer film was deposited from its chlorobenzene solution (8 mg mL^{-1}) on the substrate by spin-coating at 1500 rpm for 25 s. Before spin-coating, the polymer's chlorobenzene solution was allowed to stand on the dielectric modification layer for 20 minutes for better wetting of the surface. The obtained polymer film was annealed at 170 °C for 10 minutes in a nitrogen glove box or alternatively was not annealed. Finally, a Au source and drain electrodes were deposited on the polymer semiconductor layer through vacuum thermal evaporation. The characteristics of the OFETs were measured by a Keithley 4200 SCS semiconductor parameter analyzer under ambient conditions. The field-effect mobility (μ) was calculated by using the following equation in the saturation regime:

$$I_{DS} = \frac{WC_i}{2L}\mu(V_{GS} - V_T)^2$$

where I_{DS} is the drain current, W and L are the channel width (8800 μm) and length (80 μm), respectively, C_i is the capacitance per unit area of the gate insulator (11.1 nF cm^{-2}), V_{GS} is the gate voltage, and V_T is the threshold voltage. The transfer curve was obtained at a V_{DS} value of −60 V.

Fabrication and characterization of the polymer solar cells

The PSCs were fabricated in the configuration of the traditional sandwich structure with an indium tin oxide (ITO) glass positive electrode and a metal negative electrode. Patterned ITO glass with a sheet resistance of 10 Ω $\square^{-1}$ was purchased from CSG Holding Co. Ltd (China). The ITO glass was cleaned by sequential ultrasonic treatment in detergent, deionized water, acetone and isopropanol, then treated in an ultraviolet–ozone chamber (Ultraviolet Ozone Cleaner, Jelight Company, USA) for 20 min. The PEDOT:PSS (poly(3,4-ethylene dioxythiophene):-poly(styrene sulfonate)) (Baytron P 4083, Germany) was filtered through a 0.45 μm filter and spin coated at 2000 rpm for 60 s on the ITO electrode. Subsequently, the PEDOT:PSS film was baked at 150 °C for 15 min in the air to give a thin film with a thickness of 40 nm. A blend of the polymer and PCBM (w/w) was dissolved in *ortho*-dichlorobenzene (ODCB), and spin-cast at 3000 rpm for 45 s onto the PEDOT:PSS layer. The substrates were then dried at 70 °C for 15 min. The thickness of the photoactive layer is in the range of 70–100 nm measured by an Ambios Technology XP-2 profilometer. A bilayer cathode consisting of Ca (~20 nm) capped with Al (~100 nm) was thermally evaporated under a shadow mask with a base pressure of *ca.* 10^{-5} Pa. The active area of the PSCs is 4 mm^2. Device characterization was carried out under AM 1.5G irradiation with the intensity of 100 mW cm^{-2} (Oriel 67005, 500 W) calibrated by a standard silicon cell. *J*–*V* curves were recorded with a Keithley 236 digital source meter.

Synthesis of PBDFTT-C

M1 (0.084 g, 0.2 mmol), M2 (0.148 g, 0.2 mmol) and 15 mL of dry toluene were put into a two-necked flask. The solution was flushed with N_2 for 10 min, then $Pd(PPh_3)_4$ (15 mg) was added into the flask. The solution was flushed with N_2 again for 25 min. The oil bath was heated to 110 °C carefully, and the reactant was stirred for 24 h at this temperature under a N_2 atmosphere. Then the reaction mixture was cooled to room

temperature, and the polymer was precipitated by the addition of 100 mL of methanol and filtered through a Soxhlet thimble, which was then subjected to Soxhlet extraction with methanol, hexanes and chloroform. The polymer was recovered as a solid from the chloroform fraction by rotary evaporation. The green solid was dried under vacuum overnight (0.092 g, yield: 67%).

^{1}H NMR (400 MHz, $CDCl_3$): 7.49 (br, 1H), 7.08 (br, 2H), 4.34 (d, 4H), 3.97 (br, 1H), 2.46–1.01 (m, 26H), 0.81–0.96 (m, 18H). Anal. calcd for $(C_{40}H_{52}O_5S_2)_n$ (%): C, 70.76; H, 8.02; O, 11.78. Found (%): C, 70.43; H, 8.14; O, 11.67.

Results and discussion

Polymer synthesis

As shown in Scheme 1, the polymer was synthesized with the ditin derivative (M2) in the presence of dibromide (M1) using Stille coupling reactions.[19] The synthesized polymer was purified by continuous extraction with methanol, hexanes and chloroform, and the chloroform fractions were recovered. Gel permeation chromatography (GPC) results (using polystyrene as the standard and THF as eluent) have shown that PBDFTT-C has a average molecular weight (M_w) value of 44 KDa with a PDI of 2.1. The obtained copolymer from chloroform fractions is readily soluble in common organic solvents such as chlorobenzene, tetrahydrofuran and dichlorobenzene, *etc.*

Thermal stability

The thermal stability of the polymer is important for device applications. Fig. 1 displays the thermogravimetric (TGA) thermogram of PBDFTT-C. The TGA analysis reveals that, under the protection of an inert atmosphere, the decomposition temperature (T_d) at 5% weight loss of PBDFTT-C is 331 °C. Good thermal stability of the copolymer prevents the deformation of the copolymer morphology and the degradation of the polymeric active layer under an applied electric field.

Optical properties

The absorption spectra of PBDFTT-C in dilute $CHCl_3$ solution and the film state are shown in Fig. 2. The optical data including the absorption peak wavelength, absorption onset wavelength and the optical bandgap are listed in Table 1. The absorption spectra from dilute $CHCl_3$ solution and the film state feature two absorption bands: one at 400–450 nm, which belongs to localized π–π* transitions, and another broader band from 450 to 840 nm in the long wavelength region, corresponding to intermolecular charge transfer (ICT) between TT and BDF units. Compared to the absorption spectrum in solution, the absorption in the film became broader and red-shifted, indicating aggregation or stronger molecular interactions in the solid state. From the onset wavelength of the film absorption, we can estimate the corresponding optical bandgap of 1.48 eV for PBDFTT-C. PBDFTT-C exhibits strong and broad absorption from 500 to 840 nm, which is beneficial for obtaining high efficiency polymer solar cells.[20]

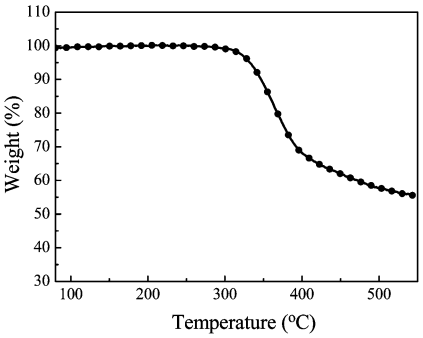

Fig. 1 TGA thermogram of PBDFTT-C with a heating rate of 20 K min^{-1}.

Electrochemical properties

To further investigate the electronic structures of the copolymer and then provide key parameters for PSC devices, it is necessary to determine the highest occupied molecular orbital (HOMO) and the lowest unoccupied molecular orbital (LUMO) levels of the copolymer.[21] The redox behavior of PBDFTT-C was investigated by cyclic voltammetry (CV) and the results were shown in Fig. 3. The HOMO and LUMO levels were estimated from the onset oxidation and reduction potentials assuming the absolute energy level of ferrocene/ferrocenium (Fc/Fc^+) to be 4.8 eV under vacuum, and the data were listed in Table 1. As a result, the HOMO and LUMO values were calculated using the equation:[22] HOMO = $-e(E_{on}^{ox} + 4.4)$ (eV); LUMO = $-e(E_{on}^{red} + 4.4)$ (eV). The

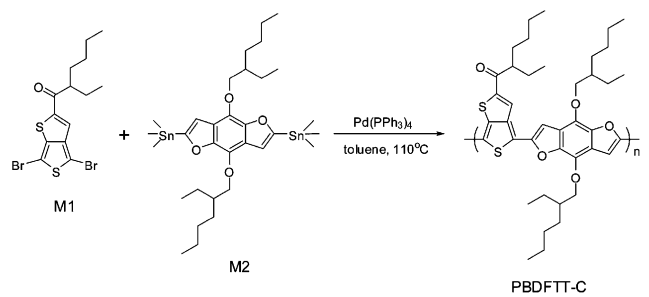

Scheme 1 Synthesis and structure of PBDFTT-C.

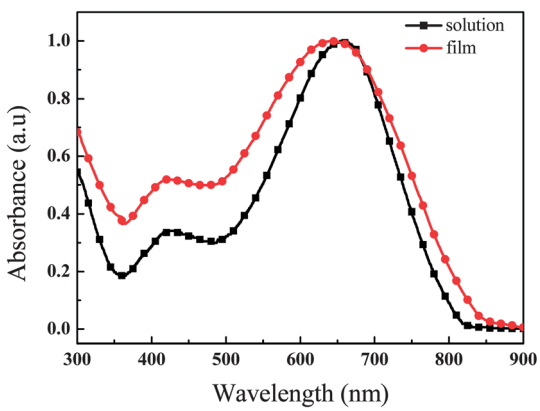

Fig. 2 UV-vis absorption spectra of PBDFTT-C in dilute $CHCl_3$ solution and in the film state.

Table 1 Optical and electrochemical properties of PBDFTT-C

	Absorption spectra				Cyclic voltammetry (*vs.* Ag/AgCl)		
	Solution[a]		Film[b]		p-doping	n-doping	—
Polymer	λ_{max} (nm)	λ_{max} (nm)	λ_{onset} (nm)	E_g^{optc} (eV)	E_{on}^{ox}/HOMO[d] (V)/(eV)	E_{on}^{red}/LUMO[d] (V)/(eV)	E_g^{EC} (eV)
PBDFTT-C	660	642	840	1.48	0.87/−5.27	−0.71/−3.69	1.58

[a] Measured in chloroform solution. [b] Cast from chloroform solution. [c] Bandgap estimated from the onset wavelength of the optical absorption. [d] HOMO = −e(E_{on}^{ox} + 4.4) (eV); LUMO = −e(E_{on}^{red} + 4.4) (eV) using Ag/AgCl as the reference electrode.

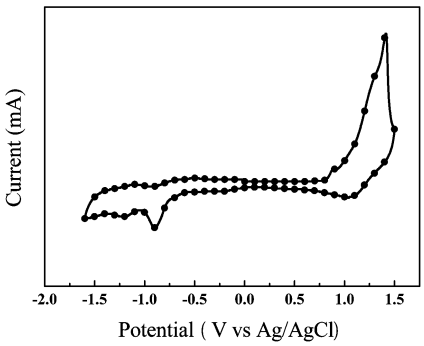

Fig. 3 Cyclic voltammogram of the PBDFTT-C film cast on a platinum disk in 0.1 M Bu_4NPF_6/CH_3CN solution at 50 mV s^{-1}.

onset reduction potential of PBDFTT-C is −0.71 V, and the corresponding LUMO energy level is −3.69 eV. The onset oxidation potential of PBDFTT-C is 0.87 V, and the corresponding HOMO energy level is −5.27 eV. The energy gap which is deduced from the electrochemical measurement is 1.58 eV for PBDFTT-C. The electrochemical bandgap of PBDFTT-C is larger than the optical bandgap due probably to the interface barrier for the charge injection from electrochemical measurement.

Hole mobility

Besides the absorption and energy levels, hole mobility is another important factor for photovoltaic applications. We investigated the hole mobility of PBDFTT-C by the space-charge-limited current (SCLC) method with a device structure of ITO/PEDOT:PSS/PBDFTT-C:$PC_{71}BM$ (1 : 1.5, w/w)/Au.[16] SCLC is described by

$$J_{SCLC} = \frac{9}{8}\varepsilon_0\varepsilon_r\mu_0\frac{(V - V_{bi})^2}{d^3}\exp\left[0.89\gamma\sqrt{\frac{V - V_{bi}}{d}}\right] \quad (1)$$

The results are plotted as $\ln(Jd^3/V^2)$ *vs.* $(V/d)^{0.5}$, as shown in Fig. 4. Here, J stands for current density, d is the thickness of the device, and $V = V_{appl} - V_{bi}$, where V_{appl} is the applied potential and V_{bi} is the built-in potential. According to eqn (1), the average hole mobility of the PBDFTT-C/$PC_{71}BM$ blend is 3.0 × 10^{-4} cm^2 V^{-1} s^{-1} among five devices. To further verify this result, we measured the hole mobility of PBDFTT-C by the FET method. Fig. 5 shows the output and transfer curves of the polymer and the corresponding characteristics after annealing at 170 °C are described in Fig. S2 in the ESI.† The related data are summarized in Table S1 in the ESI.† OFETs of PBDFTT-C afforded the hole mobility of 5.4 × 10^{-3} cm^2 V^{-1} s^{-1}. After annealing at 170 °C, the hole mobility of PBDFTT-C got improved to 7.0 × 10^{-3} cm^2 V^{-1} s^{-1}. Good hole mobility should be the result of strong π–π stacking which facilitates charge transport. In addition, further improvement of the field transfer mobility of the polymer could be achieved by using more favorable device fabrication conditions (*e.g.* different solvents, surface treatment, *etc.*). The results show that the copolymer—PBDFTT-C possesses good hole mobility up to the order of 10^{-3} cm^2 V^{-1} s^{-1}, which is beneficial to the photovoltaic performance, especially to the current density and fill factor.

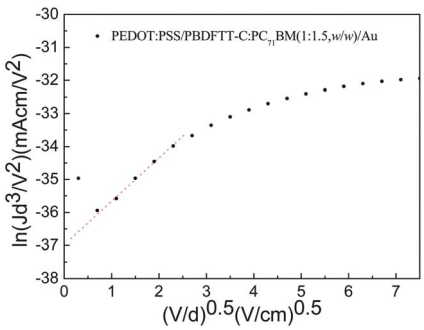

Fig. 4 $\ln(Jd^3/V^2)$ *vs.* $(V/d)^{0.5}$ plot of the PBDFTT-C blend with $PC_{71}BM$ for the measurement of the hole mobility by the SCLC method.

Photovoltaic properties

In order to investigate the potential photovoltaic applications of the polymer, the bulk heterojunction PSCs were fabricated with a device structure of ITO/PEDOT:PSS/PBDFTT-C:PCBM/Ca/Al. PSC devices were tested under simulated 100 mW cm^{-2}, AM 1.5G illumination. The typical *J*–*V* curves are demonstrated in Fig. 6 and the corresponding photovoltaic data are listed in Table 2. The photovoltaic performances of the polymer were first measured by blending with PCBM in ODCB at different weight ratios (1 : 1, 1 : 1.5 and 1 : 2). Recent studies have demonstrated that a small volume of solvent with a high boiling point, such as 1,8-diiodooctane (DIO), can be added to the BHJ system, to improve the morphology and device performance.[23] Herein, we tried DIO as a processing additive into the active layer. The photovoltaic curves and related data are described in

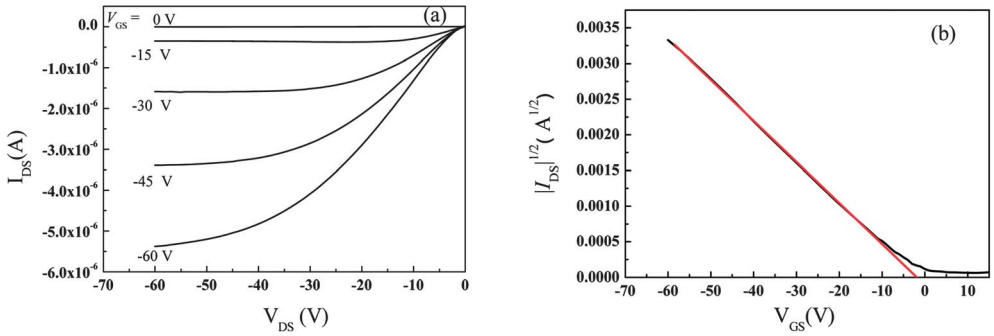

Fig. 5 Output and transfer characteristics of PBDFTT-C (a) output; (b) transfer.

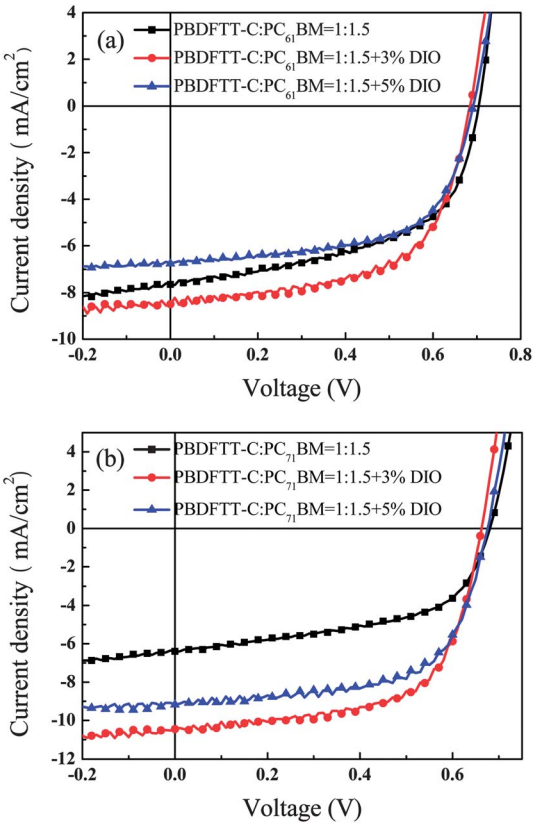

Fig. 6 *J–V* curves of the polymer solar cells based on (a) PBDFTT-C:$PC_{61}BM$ = 1 : 1.5 and PBDFTT-C:$PC_{61}BM$ = 1 : 1.5 with 3% DIO or with 5% DIO; (b) PBDFTT-C:$PC_{71}BM$ = 1 : 1.5 and PBDFTT-C:$PC_{71}BM$ = 1 : 1.5 with 3% DIO or with 5% DIO.

Table 2 Photovoltaic properties of PSCs based on PBDFTT-C:PCBM (1 : 1.5)

Active layer	V_{oc} (V)	J_{sc} (mA cm^{-2})	FF (%)	PCE (%)
PBDFTT-C:$PC_{61}BM$	0.70	7.65	54.9	2.94
PBDFTT-C:$PC_{61}BM$ + 3% DIO	0.68	8.50	60.5	3.50
PBDFTT-C:$PC_{61}BM$ + 5% DIO	0.69	6.75	61.9	2.88
PBDFTT-C:$PC_{71}BM$	0.68	6.39	54.2	2.35
PBDFTT-C:$PC_{71}BM$ + 3% DIO	0.66	10.45	63.8	4.4
PBDFTT-C:$PC_{71}BM$ + 5% DIO	0.68	9.17	63.5	3.96

detail in the ESI.† The best performance of PBDFTT-C was obtained with a donor/acceptor weight ratio of 1 : 1.5, the PCE of the PSC based on PBDFTT-C:$PC_{61}BM$ (1 : 1.5, w/w) is 2.94% with V_{oc} = 0.7 V, J_{sc} = 7.65 mA cm^{-2} and FF = 54.9 (see Fig. 6a).

Further investigations show that the PBDFTT-C based device performance can be greatly improved by the addition of DIO. As shown in Fig. 6a, with 3% DIO additive, the PCE was increased to 3.5% due to the improvement of J_{sc} and FF when PBDFTT-C was blended with $PC_{61}BM$ in the weight ratio of 1 : 1.5. Fig. 6b shows the *J–V* curves of the PSCs based on PBDFTT-C/$PC_{71}BM$ (1 : 1.5, w/w) with or without DIO. The PCE of the PSC based on PBDFTT-C:$PC_{71}BM$ (1 : 1.5, w/w) is 2.35%. The PCE was improved from 2.35% to 4.4% through the addition of 3% DIO into the active layer. The PCE of the PSC reached up to 4.4%, with a V_{oc} = 0.66 V, a J_{sc} = 10.45 mA cm^{-2} and a FF = 0.64. The nearly two-fold increase of the PCE is mainly from the higher FF and J_{sc}. With the addition of 5% DIO, the PCE decreased to 4.0% resulting from the reduction of J_{sc}. Compared to the similar benzodithiophene based polymer—PBDTTT-C, PBDFTT-C showed a deeper HOMO level, relatively higher hole mobility and a little red-shifted absorption, however, the efficiency of PBDFTT-C was lower than that of PBDTTT-C, which indicated that PCEs may still have lots of space for improvement by further device modifications.[24]

The accuracy of the photovoltaic measurements can be confirmed by the external quantum efficiency (EQE) of the devices. Fig. 7 shows the EQE plots of the PSC devices fabricated under the same conditions as those for the *J–V* measurements with PBDFTT-C:PCBM (1 : 1.5, w/w). The higher values of EQE are consistent with the higher J_{sc} measured in the solar cells. The J_{sc} values calculated from integrating the EQE data with the AM 1.5G reference spectrum are very close to that obtained from the *J–V* curves. The EQE results indicate that the photovoltaic results are credible. The EQE value of 55% at 496 nm of PBDFTT-C with 3% DIO led to a high J_{sc} which was close to *ca.* 11 mA cm^{-2}.

Morphology

The nano-scale morphology plays an important role in the device performance. Proper morphology is necessary not only for exciton dissociation but also for charge transport to respective electrodes for efficient collection.[25,26] To better

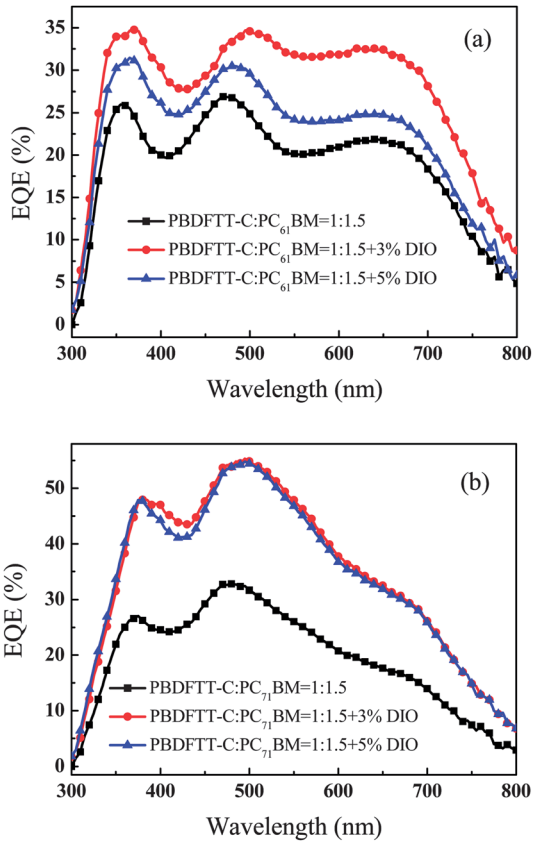

Fig. 7 The EQE curves of the PSCs based on (a) PBDFTT-C:$PC_{61}BM$ = 1 : 1.5 and PBDFTT-C:$PC_{61}BM$ = 1 : 1.5 with 3% DIO or with 5% DIO; (b) PBDFTT-C:$PC_{71}BM$ = 1 : 1.5 and PBDFTT-C:$PC_{71}BM$ = 1 : 1.5 with 3% DIO or with 5% DIO.

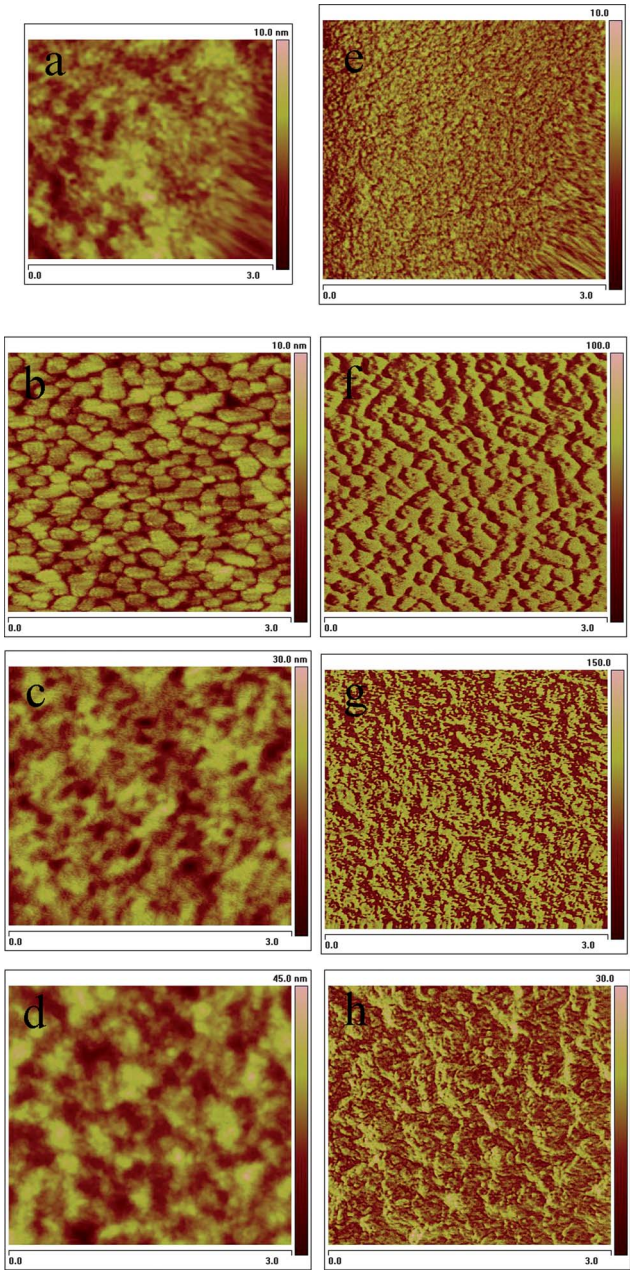

Fig. 8 AFM images of PBDFTT-C:PCBM (1 : 1.5, w/w) blend films spin coated from ODCB solutions: (a) and (e) PBDFTT-C:$PC_{61}BM$ height image and phase image; (b) and (f) PBDFTT-C:$PC_{71}BM$ height image and phase image; (c) and (g) PBDFTT-C:$PC_{71}BM$ with 3% DIO height image and phase image; (d) and (h) PBDFTT-C:$PC_{71}BM$ with 5% DIO height image and phase image.

explain the higher photovoltaic properties of PBDFTT-C:$PC_{71}BM$ = 1 : 1.5 with 3% DIO, we investigated the morphologies of PBDFTT-C and PCBM blends spin-coated from their *o*-dichlorobenzene (ODCB) solution by using tapping-mode atomic-force microscopy (AFM). Fig. 8 shows the height and phase images of PBDFTT-C:PCBM or PBDFTT-C:PCBM with 3% or 5% DIO at the optimized ratio (1 : 1.5, w/w). From the height images (Fig. 8a–d), the root-mean-square (RMS) surface roughness values of the blend films for PBDFTT-C:$PC_{61}BM$, PBDFTT-C:$PC_{71}BM$, PBDFTT-C:$PC_{71}BM$ with 3% DIO and PBDFTT-C:$PC_{71}BM$ with 5% DIO are 0.84 nm, 12.2 nm, 1.9 nm and 4.20 nm, respectively. The PBDFTT-C:$PC_{71}BM$ blend showed coarser macro-phase separation with plenty of larger crystalline round shaped aggregates and a higher RMS (12.2 nm) compared to its blend with $PC_{61}BM$, which could account for the lower PCE compared to the blend with $PC_{61}BM$ even though $PC_{71}BM$ has better absorption. The addition of 3% DIO or 5% DIO reduced the domain size and greatly improved surface roughness for polymer/PCBM blends. As a result, the J_{sc} of the devices fabricated with DIO as the processing additive were increased due to the more efficient charge generation and transport. From the phase images, PBDFTT-C:$PC_{71}BM$ with 3% or 5% DIO showed nanoscale bicontinuous phase separation morphology and good miscibility between PBDFTT-C and $PC_{71}BM$. As shown in Fig. 7f–h, the addition of DIO led to much finer phase separation, reduced domain size and the formation of an interpenetrating bicontinuous network between polymer donor and $PC_{71}BM$ with an ideal domain size of 10–20 nm, which can enhance the donor–acceptor interfacial area and improve charge generation and transportation.[25] It is obvious that the 3% DIO additive effect is more visible in the blend film, where polymer fibrillars are well distributed throughout the composite films. The improved morphology should result in a big increase in the FF and J_{sc} of the PBDFTT-C based devices with 3% DIO additive. It is firmly believed that the photovoltaic

performance of this type of copolymer can be further improved by the optimization of the film morphology and the device fabrication conditions.

Conclusion

In summary, we have synthesized a new low bandgap copolymer based on benzodifuran and a thieno-[3,4-*b*]thiophene derivative. The copolymer exhibited good solubility in common organic solvents and a broad absorption plateau from 300 nm to 840 nm. When blended with $PC_{71}BM$ in PSCs processed without additive: the low PCE is determined by a low J_{sc} and FF. When 3% DIO was used as an additive, for PBDFTT-C based devices, we measured a PCE increase to 4.4% from 2.35%, accountable to an improved film morphology for exciton generation and charge transportation. We believe the photovoltaic properties can be further improved by material design and different processing conditions.

Acknowledgements

This work was supported by NSFC (no. 51173206, 21161160443), National High Technology Research and Development Program (no. 2011AA050523), the Natural Science Foundation of Hunan Province, China (no. 11JJ4010), China Postdoctoral Science Foundation (no. 20110490150) and the Fundamental Research Funds for the Central Universities (no. 2010QZZD0112).

References

1 Y. Li, *Acc. Chem. Res.*, 2012, **45**, 723.
2 Y. Cheng, S. Yang and C. Hsu, *Chem. Rev.*, 2009, **11**, 5868.
3 Y. Li and Y. Zou, *Adv. Mater.*, 2008, **20**, 2952.
4 L. Dou, J. Gao, E. Richard, J. You, C. Chen, K. Cha, Y. He, G. Li and Y. Yang, *J. Am. Chem. Soc.*, 2012, **134**, 10071.
5 Y. Zou, A. Najari, P. Berrouard, S. Beaupré, R. Aich, Y. Tao and M. Leclerc, *J. Am. Chem. Soc.*, 2010, **132**, 5330.
6 L. Huo, S. Zhang, X. Guo, F. Xu, Y. Li and J. Hou, *Angew. Chem., Int. Ed.*, 2011, **50**, 9697.
7 B. Liu, W. Wu, B. Peng, Y. Liu, Y. He, C. Pan and Y. Zou, *Polym. Chem.*, 2010, **1**, 678.
8 (*a*) Y. He, H. Chen, J. Hou and Y. Li, *J. Am. Chem. Soc.*, 2010, **132**, 1377; (*b*) Y. He and Y. Li, *Phys. Chem. Chem. Phys.*, 2011, **13**, 1970.
9 Z. Zhang, J. Min, S. Zhang, J. Zhang, M. Zhang and Y. Li, *Chem. Commun.*, 2011, **47**, 9474.
10 C. Cui, X. Fan, M. Zhang, J. Zhang, J. Min and Y. Li, *Chem. Commun.*, 2011, **47**, 11345.
11 Y. Yao, Y. Liang, V. Shrotriya, S. Xiao, L. Yu and Y. Yang, *Adv. Mater.*, 2007, **19**, 3979.
12 H. Saadeh, L. Lu, F. He, J. Bullock, W. Wang, B. Carsten and L. Yu, *ACS Macro Lett.*, 2012, **1**, 361.
13 A. Najari, S. Beaupré, P. Berrouard, Y. Zou, J.-R. Pouliot, C. Pérusse and M. Leclerc, *Adv. Funct. Mater.*, 2011, **21**, 718.
14 (*a*) Y. Liang, D. Feng, Y. Wu, S. Tsai, G. Li, C. Ray and L. Yu, *J. Am. Chem. Soc.*, 2009, **131**, 7792; (*b*) H. Chen, J. Hou, S. Zhang, Y. Liang, G. Yang, Y. Yang, L. Yu, Y. Wu and G. Li, *Nat. Photonics*, 2009, **3**, 649.
15 L. Huo, Y. Huang, B. Fan, X. Guo, Y. Jing, M. Zhang, Y. Li and J. Hou, *Chem. Commun.*, 2012, **48**, 3318.
16 X. Chen, B. Liu, Y. Zou, L. Xiao, X. Guo, Y. He and Y. Li, *J. Mater. Chem.*, 2012, **22**, 17724.
17 J. Hou, H. Chen, S. Zhang, R. Chen, Y. Yang, Y. Wu and G. Li, *J. Am. Chem. Soc.*, 2009, **131**, 15586.
18 X. Xu, B. Liu, Y. Zou, Y. Guo, L. Li and Y. Liu, *Adv. Funct. Mater.*, 2012, DOI: 10.1002/adfm.201200316.
19 (*a*) J. Hou, Z. Tan, Y. Yan, Y. He, C. Yang and Y. Li, *J. Am. Chem. Soc.*, 2006, **128**, 4911; (*b*) E. Zhou, Z. Tan, L. Huo, Y. He, C. Yang and Y. Li, *J. Phys. Chem. B*, 2006, **110**, 26062.
20 J. Chen and Y. Cao, *Acc. Chem. Res.*, 2009, **42**, 1709.
21 S. Park, A. Roy, S. Beaupré, S. Cho, N. Coates, J. Moon, D. Moses, M. Leclerc, K. Lee and A. Heeger, *Nat. Photonics*, 2009, **3**, 297.
22 C. Duan, W. Cai, F. Huang, J. Zhang, M. Wang, T. Yang, C. Zhong, X. Gong and Y. Cao, *Macromolecules*, 2010, **43**, 5262.
23 J. K. Lee, W. L. Ma, C. J. Brabec, Y. Yuen, J. S. Moon, J. Y. Kim, K. Lee, G. C. Bazan and A. J. Heeger, *J. Am. Chem. Soc.*, 2008, **130**, 3649.
24 J. Hou, H. Chen, S. Zhang, R. Chen, Y. Yang, Y. Wu and G. Li, *J. Am. Chem. Soc.*, 2009, **113**, 15586.
25 T. Chu, J. Lu, S. Beaupré, Y. Zhang, J. Pouliot, S. Wakim, J. Zhou, M. Leclerc, Z. Li, J. Ding and Y. Tao, *J. Am. Chem. Soc.*, 2011, **133**, 4250.
26 W. Li, Y. Zhou, B. V. Andersson, L. M. Andersson, Y. Thomann, C. Veit, K. Tvingstedt, R. Qin, Z. Bo, O. Inganas, U. Würfel and F. Zhang, *Org. Electron.*, 2011, **12**, 1544.

